APPENDIX X

MATES V

DRAFT REPORT

Spatial and Temporal Trends of PM2.5 and TSP Components in the South Coast Air Basin

Appendix X

Spatial and Temporal Trends of PM2.5 and TSP Components in the South Coast Air Basin (An Update from MATES IV)

X.1. Overview

While particulate pollution has decreased significantly over the past decades in the South Coast Air Basin (SCAB), exposure to airborne particulate matter and toxic species within particulate matter continues to pose significant health risks for South Coast residents. In order to better understand long-term trends in particulate matter concentration and composition, fine particulate matter ($PM_{2.5}$) and total suspended particulate (TSP) samples were collected and analyzed at ten MATES V sites throughout the SCAB as in previous MATES campaigns. This appendix discusses findings from MATES V $PM_{2.5}$ and TSP analysis with particular attention to trends between MATES IV (2012-2013) and MATES V (2018-2019).

$PM_{2.5}$ mass reconstructions at five MATES V sites showed similar patterns to results from MATES IV, with organic matter making up the largest fraction (45-48%) of $PM_{2.5}$ mass, followed by the combined secondary inorganic ion fraction (ammonium sulfate and ammonium nitrate, 37-41%). Seasonal trends in reconstructed $PM_{2.5}$ component concentrations were also largely consistent with those observed in MATES IV, with fall/winter maxima in elemental carbon and ammonium nitrate, summer maximum in ammonium sulfate, and less seasonally distinct or more complex patterns in other components. Elemental carbon levels throughout the SCAB dropped substantially between MATES IV and MATES V, with 31-64% reductions at all ten MATES V sites. Ambient toxic metal concentrations measured in TSP samples showed mixed trends by metal and site. Hexavalent chromium, nickel, and lead concentrations decreased at most sites between MATES IV and MATES V (29, 21, and 17% decreases in basin averages, respectively), while cadmium levels increased at most sites (114% increase in basin average). Trends for other toxic metals, including arsenic, manganese, antimony, cobalt, and chromium, were highly spatially variable with more muted changes in overall basin averages.

X.2. Mass Reconstruction of $PM_{2.5}$

$PM_{2.5}$ consists of a wide range of inorganic and organic species, reflecting diverse sources and complex aerosol chemical processes. $PM_{2.5}$ can be broadly grouped into five major components: elemental carbon (EC), organic matter (OM), secondary inorganic ions (ammonium, nitrate, and sulfate), sea salt, and crustal/soil material. Mass reconstruction of $PM_{2.5}$ from estimated contributions of these components is commonly performed to evaluate consistency between different chemical analyses as well as to assess temporal and spatial variability in $PM_{2.5}$ composition. In the MATES IV study, mass reconstruction calculations showed generally similar $PM_{2.5}$ composition across the SCAB, with organic matter and secondary inorganic ions as the dominant fractions (42-46% and 34-38% of average reconstructed mass across all sites, respectively) (South Coast AQMD 2015). To assess changes in $PM_{2.5}$ composition since the MATES IV period (July 2012-June 2013), this exercise was repeated for the five MATES V sites

(Anaheim, Central Los Angeles, Inland Valley San Bernardino, Long Beach, and Rubidoux) where the full suite of $PM_{2.5}$ measurements was available.

Mass reconstruction calculations were performed for $PM_{2.5}$ samples collected on a 1-in-6 day schedule from May 2018 through April 2019. Since reconstructed masses were calculated for each MATES V sample (i.e., single observations), concentrations were used as reported without any detection limit censoring. Estimated contributions of each $PM_{2.5}$ component were calculated according to guidance for the EPA Chemical Speciation Network (Air Quality Research Center, University of California, Davis 2019). The only deviation from this guidance was to estimate ammonium sulfate from sulfate ion data measured by ion chromatography (IC) instead of sulfur measured by X-Ray Fluorescence (XRF). Staff made this substitution was due to possible negative bias in XRF data caused by instrumental issues during analysis of MATES V samples.

Two of the components (secondary inorganic ions and sea salt) were calculated with different formulas than those used in MATES IV (see Table 1). The change in the secondary inorganic ions formula resulted in minimal differences in calculated fractions (1-6% difference in site averages). However, the change in sea salt formula did result in significantly lower sea salt fractions (reductions of 0.18-0.55 ug/m^3, 39-64% in calculated site averages). Calculating sea salt from only chloride ion data may underestimate total sea salt due to chlorine loss from sea salt aerosols during transport (Chow, et al. 2015). However, the alternative formula (sum of sodium and chloride ions) was not used in this study due to uncertainty associated with relatively high sodium concentrations measured on field blank filters. For consistency in comparing MATES IV and MATES V results, MATES IV inorganic ion and sea salt fractions were recalculated with the updated formulas in Table X-1.

Overall, reconstructed and measured filter $PM_{2.5}$ masses for all MATES V samples showed good agreement ($r^2 = 0.84$, n = 289). The average ratio of reconstructed mass to measured mass for all samples was 0.99 ± 0.20 (1σ), with the lowest average ratio at Long Beach (0.88 ± 0.21) and highest at Inland Valley San Bernardino (1.09 ± 0.20). As discussed extensively in Chow et al. (2015), the largest sources of uncertainty in the mass reconstruction calculation include sampling artifacts, analytical uncertainty, and scaling factors used to calculate component contributions, particularly the organic matter/organic carbon scaling factor. There is also some uncertainty associated with using concentrations below detection limits in mass reconstruction calculations. In order to assess the size of this effect, potential concentration ranges for each component were calculated by substituting zero and minimum detection limit concentrations for non-detects to calculate lower and upper limits, respectively. These calculations showed that uncertainty in non-detect concentrations had a very minimal effect on average reconstructed mass (less than 2% or 0.15 ug/m^3). The effect of non-detects was most pronounced for sea salt, where calculated five-site averages for zero-substituted, uncensored, and MDL-substituted data were 0.18, 0.29, and 0.34 ug/m^3, respectively.

Figure X-1 shows mass balances by site for both MATES IV and MATES V. Site to site comparisons between MATES IV and MATES V are also provided in Table X-2. As in MATES IV, OM was the largest fraction of reconstructed mass at all sites (45-48%), followed by the

combined secondary inorganic ion fraction (37-41%). The most notable changes from MATES IV to MATES V were the reductions in ammonium sulfate and EC fractions. Average sulfate concentrations decreased from MATES IV to MATES V at all five sites by 18-23%. Since sulfate aerosols in the SCAB are mostly derived from burning of sulfur-containing fuels (including both land-based and ocean-going vessel fuel combustion), the uniform reduction in $PM_{2.5}$ sulfate points to reduced sulfur emissions from these sources. EC concentrations dropped substantially at all five sites (40-49% decrease from MATES IV concentrations), also pointing to reduced diesel emissions. EC trends throughout the SCAB are discussed in further detail in Section X.3. Average OM also decreased slightly at all five sites (4-17% decrease from MATES IV concentrations), while ammonium nitrate, crustal material, and sea salt fractions generally remained at similar levels to those calculated in MATES IV.

Seasonal $PM_{2.5}$ concentration and composition patterns are controlled by a combination of meteorological conditions (e.g., temperature, wind direction and speed, solar radiation/actinic flux, atmospheric mixing height) and source changes (e.g., winter wood burning, vegetation growth, wildfires). Figure X-2a shows monthly averages for each $PM_{2.5}$ component, reconstructed mass, and measured mass for the five sites across the MATES V measurement period. Both reconstructed and measured mass showed similar temporal trends, with generally higher values from June to December.

The variable seasonal patterns of calculated $PM_{2.5}$ components were generally consistent with trends observed in MATES IV (Figure X-2b). EC showed clear fall/winter maxima at all sites, likely due to favorable meteorological conditions for particle accumulation, as well as contributions from winter wood burning. OM had a less pronounced seasonal cycle, with inland sites (Inland Valley San Bernardino and Rubidoux) showing summer maxima, Central LA peaking in fall, and Anaheim and Long Beach peaking in winter. The variable OM seasonal signals reflect the balance between complex meteorological and source effects at different sites through the year, including increased secondary organic aerosol formation in the summer, cooler temperatures and meteorological conditions favorable for increased particle accumulation in the winter, and seasonal sources of organic matter (e.g., winter wood burning, see Appendix XII). It is important to note that two wildfire events may have had significant effects on OM monthly averages. As evidenced by elevated levoglucosan concentrations and High Resolution Rapid Refresh (HRRR) smoke model forecasts, a smoke plume from wildfires in northern California likely contributed to the highest basin-wide OM concentration of the MATES V period on August 24, 2018, while smoke from the Woolsey/Hill Fires likely contributed to high OM in November 10, 2018 samples.

Ammonium nitrate and ammonium sulfate fractions showed distinct but opposing seasonal signals. The calculated ammonium nitrate fraction peaked in the fall/winter at all five sites (average winter concentrations: 3.03-4.11 ug/m^3, 1.5-3.2x summer concentrations), while ammonium sulfate peaked in the summer (average summer concentrations: 2.48-2.86 ug/m^3, 3.5-5.8x winter concentrations). These seasonal trends largely reflect meteorological controls on sulfate and nitrate particle chemistry: increased actinic flux during the summer drives photochemical oxidation of sulfur dioxide and sulfate particle formation, while cooler winter

temperatures favor nitrate particle formation from gaseous nitric acid (Seinfeld and Pandis 2016).

Both sea salt and crustal material showed generally muted seasonal variability. Seasonal differences in crustal material were more pronounced at inland sites, with summer/fall (June-November) averages (Rubidoux 1.36 ug/m^3, Inland Valley San Bernardino: 1.39 ug/m^3) nearly double the winter/spring (December-May) averages (Rubidoux: 0.76 ug/m^3, Inland Valley San Bernardino: 0.78 ug/m^3). Unlike in MATES IV where calculated sea salt fractions peaked in the summer, sea salt concentrations were slightly lower in the summer compared to the rest of the year. However, this difference was driven by the change in sea salt formula, as recalculated MATES IV data do not show higher summer values. In general, the true sea salt contribution to $PM_{2.5}$ is difficult to estimate due to uncertainty in calculation parameters, as well as the high fraction of chloride results near or below instrument detection limits.

Table X-1. Summary of mass balance reconstruction calculations in MATES IV and MATES V. MATES V formulas are based on current guidance for EPA Chemical Speciation Network (Air Quality Research Center, University of California, Davis 2019). Differences between the studies are highlighted in bold.

Component	MATES IV	MATES V
Elemental carbon	As reported	As reported
Organic matter	1.4 × organic carbon	1.4 × organic carbon
Secondary inorganic ions	**Ammonium + sulfate + nitrate**	**Ammonium nitrate = 1.29 × nitrate** **Ammonium sulfate = 1.375 × sulfate**
Sea salt	**Sodium + chloride**	**1.8 × chloride**
Crustal material	2.2 × aluminum + 2.49 × silicon + 1.63 × calcium + 2.42 × iron + 1.94 × titanium	2.2 × aluminum + 2.49 × silicon + 1.63 × calcium + 2.42 × iron + 1.94 × titanium

Table X-2. Site comparisons of annual average concentrations of calculated $PM_{2.5}$ components, reconstructed mass, and measured mass between MATES IV (July 2012 – June 2013) and MATES V (May 2018 – April 2019). The contribution of each component to overall average reconstructed mass is shown in parentheses. Note that MATES IV ammonium nitrate, ammonium sulfate, and sea salt concentrations were recalculated with updated formulas. All concentrations are in ug/m^3.

Component	Central Los Angeles		Long Beach*		Anaheim		Inland Valley S.B.		Rubidoux	
	MATES IV	MATES V	MATES IV	MATES V	MATES IV	MATES V	MATES IV	MATES V	MATES IV	MATES V
Elemental carbon	1.23 (9%)	0.71 (6%)	0.90 (8%)	0.48 (5%)	0.90 (8%)	0.46 (5%)	1.36 (9%)	0.73 (5%)	1.11 (8%)	0.66 (5%)
Organic matter	6.25 (45%)	5.97 (48%)	5.03 (45%)	4.23 (45%)	5.24 (47%)	4.48 (45%)	6.77 (46%)	6.50 (48%)	6.47 (46%)	5.81 (47%)
Ammonium nitrate	3.27 (23%)	3.00 (24%)	2.13 (19%)	2.12 (22%)	2.11 (19%)	2.44 (25%)	3.23 (22%)	3.37 (25%)	3.58 (25%)	3.18 (26%)
Ammonium sulfate	2.12 (15%)	1.75 (14%)	2.20 (20%)	1.74 (18%)	2.01 (18%)	1.55 (16%)	1.94 (13%)	1.56 (12%)	1.82 (13%)	1.45 (12%)
Sea salt	0.29 (2%)	0.31 (2%)	0.32 (3%)	0.38 (4%)	0.26 (2%)	0.31 (3%)	0.20 (1%)	0.22 (2%)	0.20 (1%)	0.24 (2%)
Crustal material	0.84 (6%)	0.71 (6%)	0.63 (6%)	0.56 (6%)	0.62 (6%)	0.64 (6%)	1.17 (8%)	1.10 (8%)	0.86 (6%)	1.05 (8%)
Reconstructed $PM_{2.5}$ Mass	14.01	12.44	11.20	9.50	11.14	9.88	14.67	13.48	14.05	12.38
Measured $PM_{2.5}$ Mass	14.14	12.43	12.95	10.88	12.37	10.60	14.33	12.55	13.83	12.50

*Station location moved from MATES IV to MATES V.

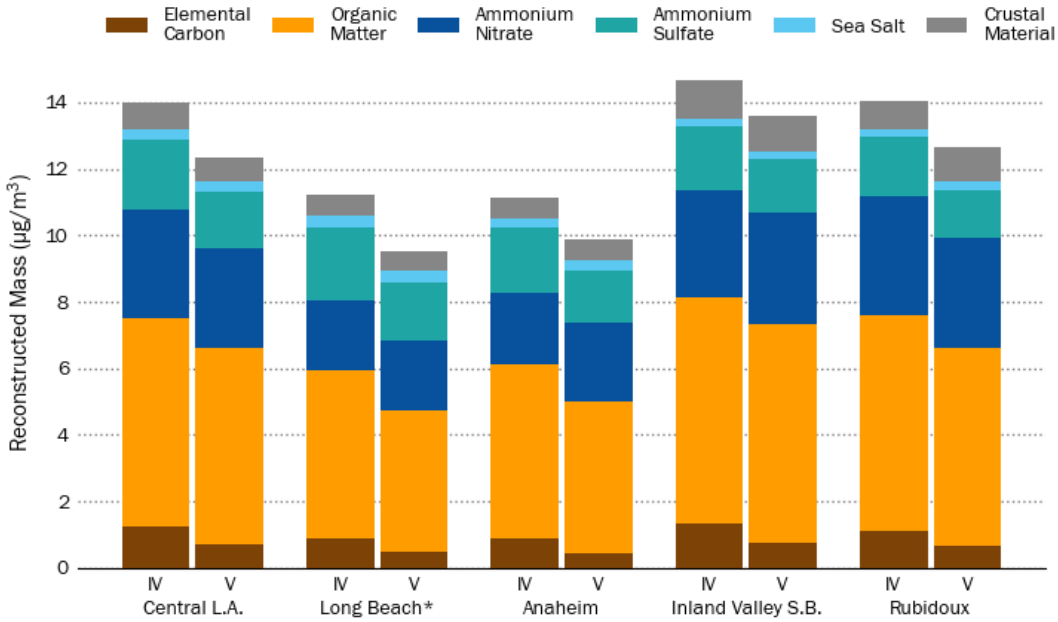

Figure X-1. Average reconstructed $PM_{2.5}$ compositions at five sites in the South Coast Air Basin during MATES IV (July 2012-June 2013) and MATES V (May 2018-April 2019). Asterisk indicates station location moved between MATES IV and V campaigns.

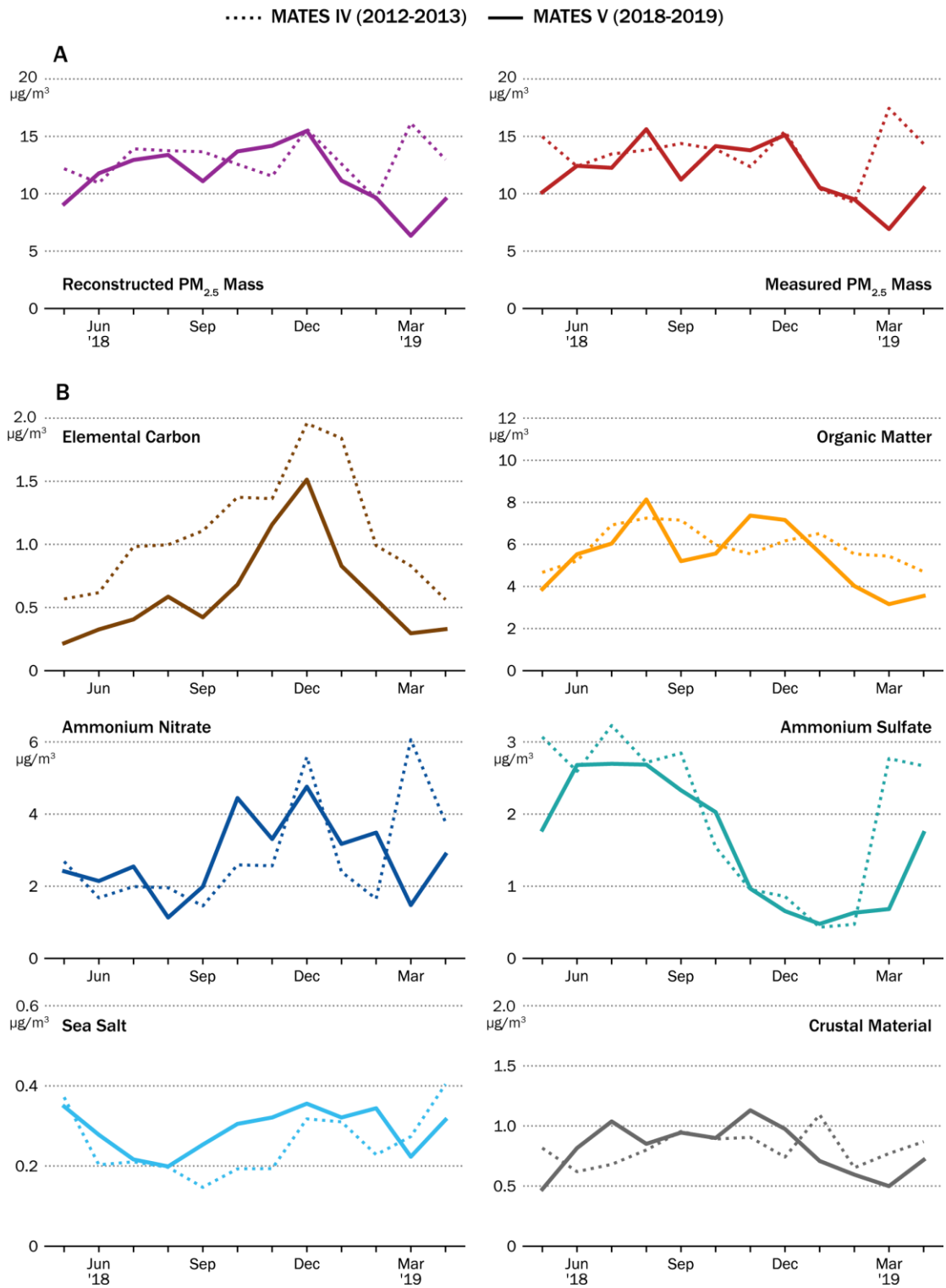

Figure X-2. a. Monthly averages of reconstructed and measured $PM_{2.5}$ mass during MATES V. b. Monthly averages of calculated $PM_{2.5}$ components during MATES V. Bold lines show MATES V five-site (Anaheim, Central L.A., Long Beach, Inland Valley San Bernardino, Rubidoux) averages and dotted lines show MATES IV five-site averages.

X.3. Elemental Carbon in PM2.5

Elemental carbon (EC) is a byproduct of combustion processes, including diesel and gasoline engine combustion, wildfire, and residential wood burning. Critically, $PM_{2.5}$ EC concentrations are currently used to estimate diesel particulate matter, which is the largest contributor to air toxics cancer risk in the SCAB (67.3% of total MATES V population-weighted average cancer risk). EC concentrations were measured in $PM_{2.5}$ samples collected on 1-in-6 day schedule at all ten fixed MATES V sites. Black carbon (BC), a closely related but distinct species from EC, was also measured on a continuous basis at all sites and is discussed in more detail in Chapter 5 and Appendix VI.

The average $PM_{2.5}$ EC concentration across all monitoring stations during MATES V was 0.64 ± 0.05 µg/m^3, which was 45% lower than the MATES IV basin-wide station average. Average EC concentrations at each site ranged from 0.46 µg/m^3 at Anaheim to 0.75 µg/m^3 at Inland Valley San Bernardino. Figure X-3 shows EC concentrations decreased at each individual site compared to MATES IV levels, ranging from a 31% drop at Compton to a 64% drop at the Burbank Area station, although the Burbank Area station was relocated between MATES IV and V. Furthermore, basin-wide monthly average concentrations were consistently lower in MATES V (Figure X-4). Decreases in monthly average concentrations between MATES IV and MATES V ranged from 19% in November to 63% in September. As observed in MATES IV, EC concentrations at all sites were generally higher in fall/winter compared to spring/summer due to a combination of meteorological conditions and some contribution from residential wood burning. The relative magnitude of the seasonal cycle also remained similar between MATES IV and MATES V, with a ratio of average winter (December-February) basin-wide EC concentration to average summer (June-August) concentration of 2.3 in MATES IV and 2.4 in MATES V.

The uniform spatial and temporal decreases in EC concentrations in the SCAB between MATES IV and MATES V point to continued reductions in EC emissions across the basin, which is consistent with a 56% reduction in total $PM_{2.5}$ EC emissions in the MATES V (2018) emissions inventory compared to the MATES IV (2012) inventory (see Appendix VIII). The overall reduction in EC emissions was driven by large reductions across stationary sources (-58%), on-road vehicles (-69%), and other mobile sources (-38%).

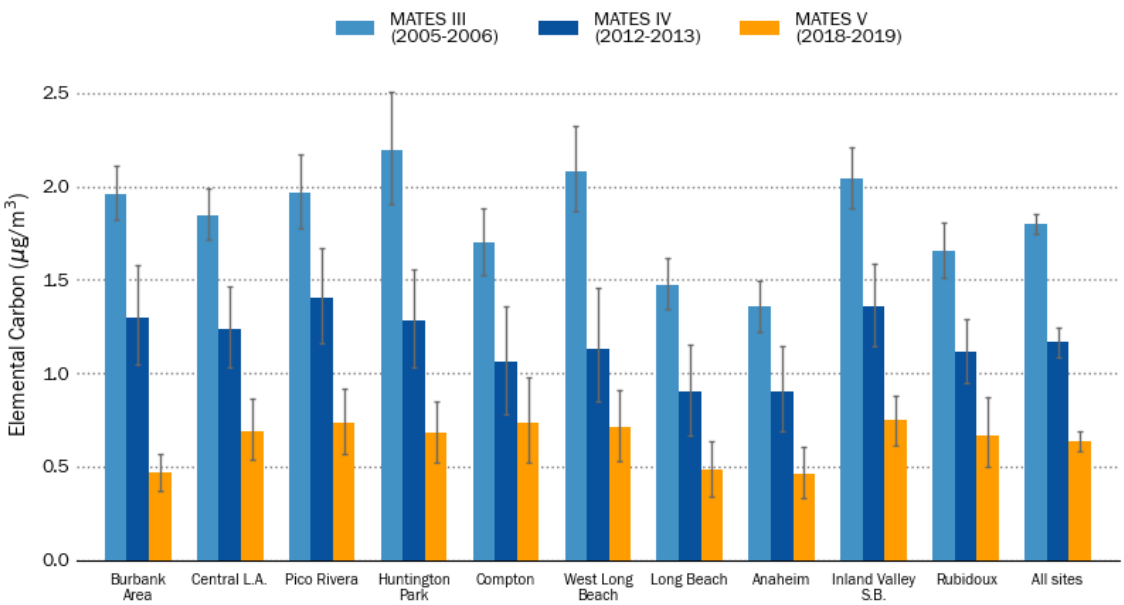

Figure X-3. Kaplan-Meier mean $PM_{2.5}$ elemental carbon concentrations from MATES III to MATES V. Error bars indicate 95% confidence intervals.

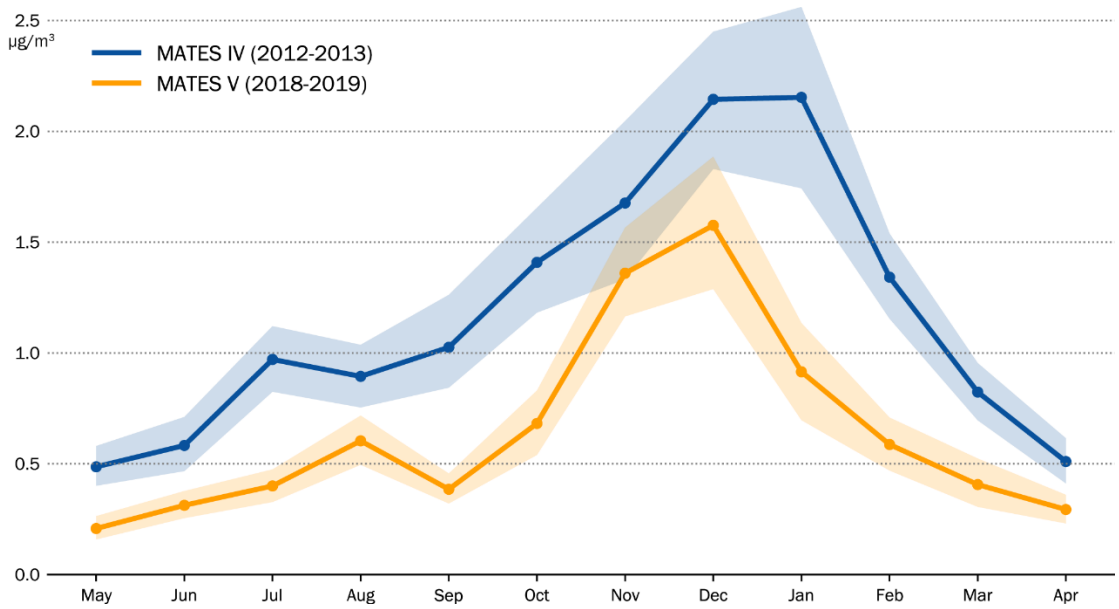

Figure X-4. Comparison of basin-wide station average $PM_{2.5}$ concentrations by month during MATES IV (2012-2013) and MATES V (2018-2019). Shading indicates 95% confidence intervals.

X.4. Metals in TSP

As in previous MATES studies, ambient toxic metal concentrations in the SCAB were assessed by analysis of total suspended particulate (TSP) samples, which incorporate both coarse and fine particulate matter fractions. Figures X-5 through X-12 show average MATES V TSP metal concentrations compared to MATES IV levels. Overall, metal air toxics contribute to approximately 10.4% of population-weighted average multi-pathway cancer risk in the SCAB. The metal species with the largest contributions to total population-weighted MATES V air toxics cancer risk are arsenic (6.4% of total risk) and hexavalent chromium (2.5%). Other metal air toxics' contribution to overall population-weighted cancer risk include cadmium (0.9%), nickel (0.4%), and lead (0.2%). Given the relatively small contribution of each of these metal air toxics to the overall air toxics cancer risk, small changes in the measured levels would not have a large impact on the cancer risk contribution from that pollutant. However, in the exploratory analysis of chronic non-cancer risk based on the measurement data, arsenic was identified as contributing to about 50% of this risk (Chapter 2). Therefore, changes in arsenic levels may impact the overall chronic non-cancer risk. Concentrations of these metals measured at fixed monitoring stations showed mixed trends from MATES IV to MATES V (Figure X-13).

The ten-station average arsenic concentration showed virtually no change from MATES IV, with increases in average concentration observed at three sites (West Long Beach, Anaheim, Pico Rivera) and similar or decreased concentrations at other sites. The increase in average concentration at West Long Beach was driven by one extreme outlier on July 19, 2018 (20.3 ng/m^3); construction activities were occurring at this monitoring station immediately adjacent to the sampling equipment, and PM levels were extremely high. Increased levels of arsenic at Anaheim and Pico Rivera were more distributed through the year. An analysis of arsenic concentrations from monitoring locations throughout the US showed that the concentrations detected in the MATES V sites were similar to concentrations elsewhere in the US (see Appendix IV, Figure IV-75). Arsenic concentrations were strongly correlated with a number of other metal species at all sites, including manganese (r^2 range of 0.60-0.94, N = 57-60), titanium (r^2 = 0.61-0.92, N = 57-60), vanadium (r^2 = 0.61-0.90, N= 35-45), chromium (r^2 = 0.52-0.86, N = 58-61), and barium (r^2 = 0.54-0.81, N= 51-56).[1] These correlations are consistent with mixed sources of arsenic in the SCAB, including crustal material, abrasive vehicle emissions, and industrial emissions, as found in Pakbin et al. (2011). Arsenic, manganese, titanium, and vanadium all showed higher concentrations in the summer/fall at inland sites compared to other sites, which is consistent with increased crustal dust during warmer and drier months.

Hexavalent chromium concentrations decreased at most sites, with a 29% decrease in the basin-wide average from MATES IV to MATES V. The only substantial increase was at Anaheim where average concentrations increased from 0.027 to 0.038 ng/m^3 (+43%) but remained below the MATES V basin-wide average of 0.040 ng/m^3. As observed in MATES IV, average hexavalent chromium concentrations were highest at Compton (0.061 ng/m^3) and Huntington Park (0.057 ng/m^3), although average concentrations decreased substantially compared to MATES IV (-46% at both sites). Compared to other MATES stations, these two stations are

[1] All $p << 0.001$. One extreme outlier was removed at West Long Beach since r^2 values were artificially inflated.

located closer to a number of metal-processing facilities that handle hexavalent chromium. South Coast AQMD has conducted special monitoring investigations and enforcement efforts in communities where a large number of hexavalent chromium emitting facilities are located, and continue to develop and/or amend regulations to control these types of metal emissions. Hexavalent chromium concentrations did not show any strong correlation with other measured TSP metals, which is consistent with distinct or highly variable sources in the SCAB.

Average cadmium concentrations increased at most sites, with very large increases at West Long Beach (+ 507%), Rubidoux (+348%), and Burbank Area (+415%). At the Burbank Area station, this increase was largely driven by one extremely high sample (30 ng/m^3) on December 22, 2018, but increases in average concentrations at other sites could not be attributed to any one outlier. Similar to hexavalent chromium, cadmium concentrations did not show strong correlations with any other measured metals across the basin, pointing to distinct or heterogeneous sources.

Basin-wide average concentrations of nickel and lead both declined from MATES IV to MATES V, but trends at individual sites varied. While average nickel concentrations decreased substantially at some sites, the average concentration at Inland Valley San Bernardino rose by 55% compared to MATES IV. Much of the observed increase at Inland Valley San Bernardino was driven by a series of high concentration samples during the summer (June-August). Nickel is also of interest as a tracer of emissions from heavy fuel oil combustion by ocean-going vessels (OGV) (Agrawal, et al. 2009). The usage of heavy fuel oil fuel should have been phased out by OGVs with the low sulfur fuel requirements implemented by the California Air Resources Board[2] and the International Maritime Organization[3] over the past decade. At the two sites near the ports, West Long Beach and Long Beach, nickel concentrations increased by 16% and 1%, respectively. However, nickel concentrations at these sites were not significantly correlated ($r^2 = 0.04$, $p > 0.05$), pointing to the importance of local sources and meteorological patterns. Lead concentrations decreased across the SCAB from MATES IV to MATES V by 21-39%, with the exception of Anaheim and Burbank Area stations, where average lead concentrations increased by 30% and 28%, respectively. Average lead concentrations at every site (2.72-7.66 ng/m^3) were well below the National Ambient Air Quality Standard for lead (150 ng/m^3 average over 3 months). Furthermore, every sample measured during MATES V remained below this standard, with the highest individual sample concentration (106.4 ng/m^3) recorded at Huntington Park on April 15, 2019.

Other metals designated as Hazardous Air Pollutants by the EPA and measured as part of MATES V include manganese, antimony, chromium, cobalt, beryllium, and selenium. Temporal trends in these metals, except for beryllium and selenium, are shown in Figures X-5 through X-12 and Figure X-13. Selenium and beryllium concentrations were generally too low to be reliably quantified (77% of MATES V samples were below detection limit for selenium, and 76% were below detection limit for beryllium), so true ambient trends were difficult to discern.

[2]For more information, see https://ww2.arb.ca.gov/our-work/programs/ocean-going-vessel-fuel-regulation
[3]For more information, see https://www.imo.org/en/MediaCentre/PressBriefings/Pages/34-IMO-2020-sulphur-limit-.aspx

Basin-wide average concentrations of manganese, antimony, and cobalt increased from MATES IV averages (+11, 4, 18%, respectively), while average chromium concentration declined slightly (-8%). Trends at individual sites varied considerably. While concentrations of these metals uniformly decreased at Central Los Angeles and Huntington Park, concentrations increased at West Long Beach and Anaheim. Anaheim in particular showed higher concentrations of nearly every measured TSP metal from MATES IV and MATES V. Since the Anaheim station location and sampling method did not change between the two studies, this trend could be the result of changes in local sources and/or particle transport to this site. Other noteworthy increases include the average cobalt concentration at Long Beach, which doubled between MATES IV (0.37 ng/m^3) to MATES V (0.75 ng/m^3). This increase was primarily driven by high winter concentrations and could reflect closer proximity to a local cobalt source due to the change in the Long Beach station location between MATES IV and MATES V sampling campaigns. Cobalt concentrations at Long Beach were strongly correlated with nickel (r^2 = 0.93) and chromium (r^2 = 0.79), suggesting a possible common source of these metals at this site.

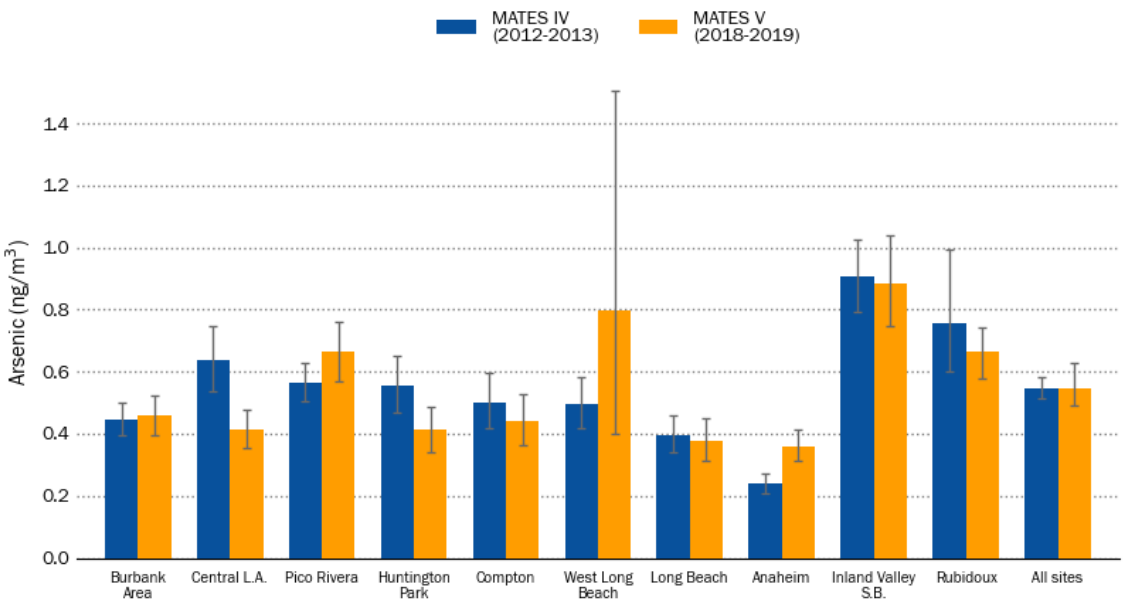

Figure X-5. Kaplan-Meier mean TSP arsenic concentrations by site during MATES IV (2012-2013) and MATES V (2018-2019). Error bars indicate 95% confidence intervals.

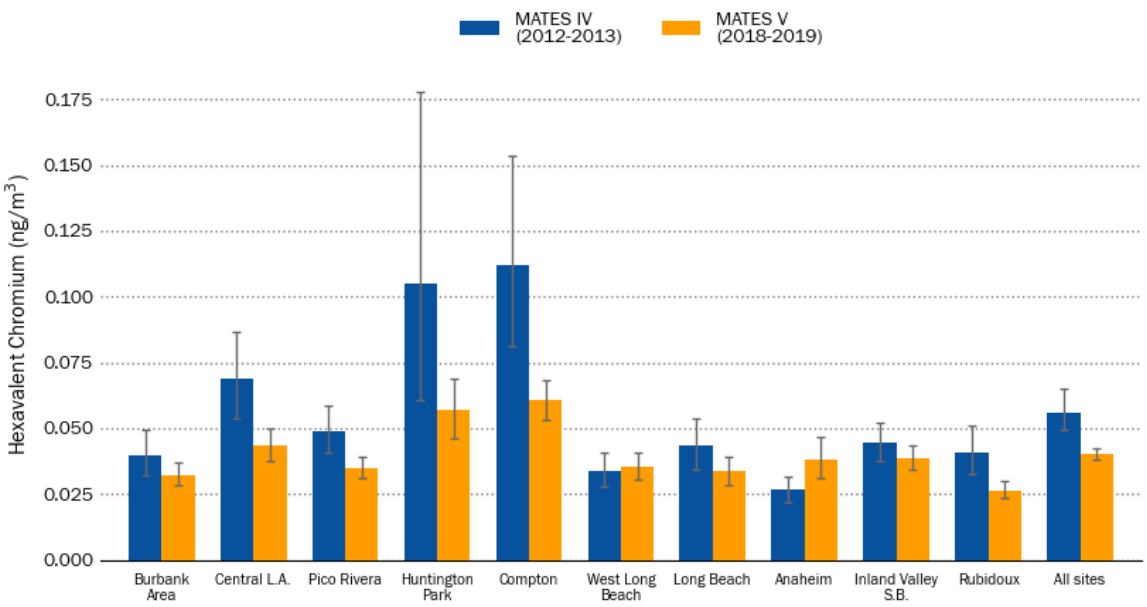

Figure X-6. Kaplan-Meier mean TSP hexavalent chromium concentrations by site during MATES IV (2012-2013) and MATES V (2018-2019). Error bars indicate 95% confidence intervals.

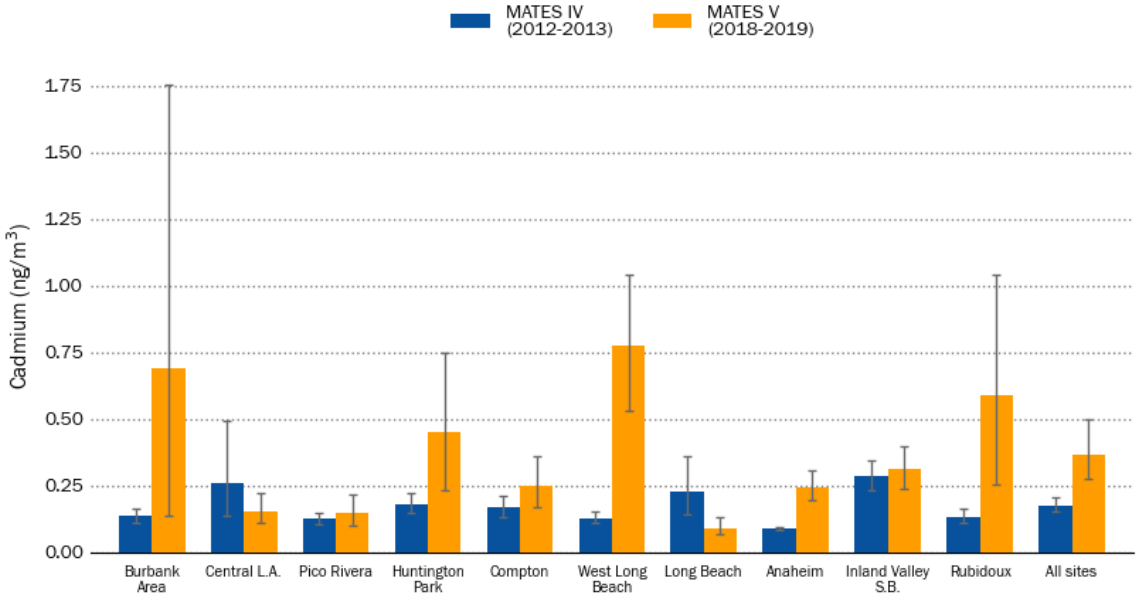

Figure X-7. Kaplan-Meier mean TSP cadmium concentrations by site during MATES IV (2012-2013) and MATES V (2018-2019). Error bars indicate 95% confidence intervals.

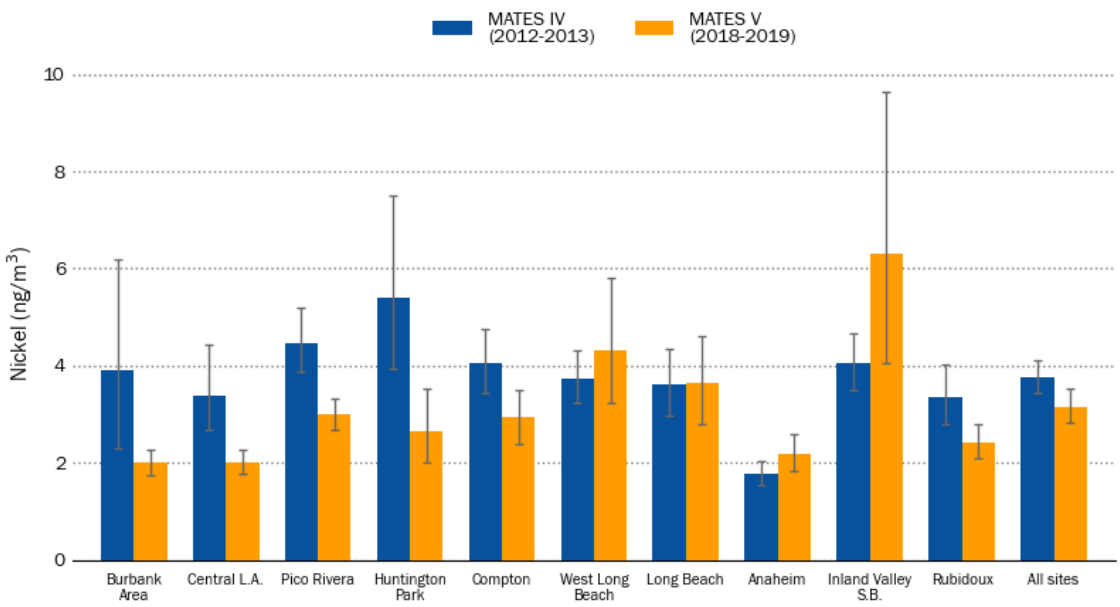

Figure X-8. Kaplan-Meier mean TSP nickel concentrations by site during MATES IV (2012-2013) and MATES V (2018-2019). Error bars indicate 95% confidence intervals.

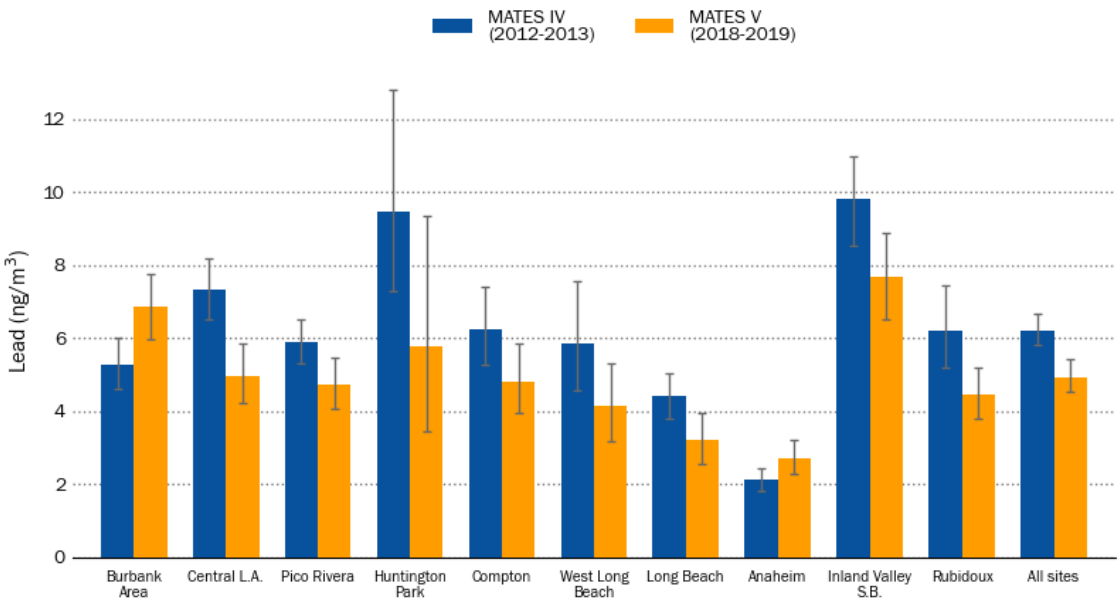

Figure X-9. Kaplan-Meier mean TSP lead concentrations by site during MATES IV (2012-2013) and MATES V (2018-2019). Error bars indicate 95% confidence intervals.

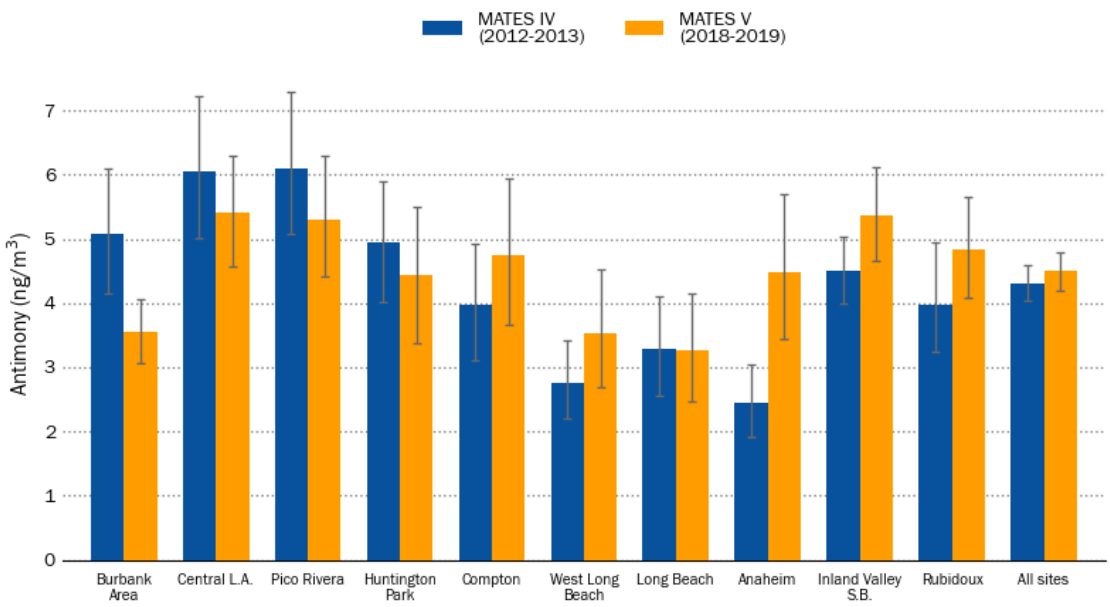

Figure X-10. Kaplan-Meier mean TSP antimony concentrations by site during MATES IV (2012-2013) and MATES V (2018-2019). Error bars indicate 95% confidence intervals.

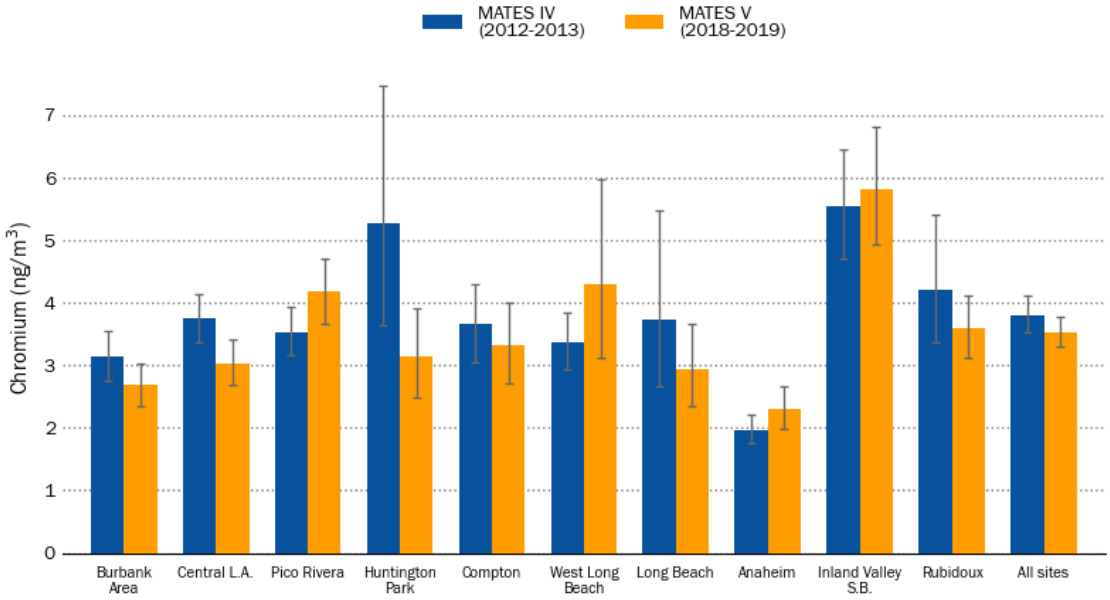

Figure X-11. Kaplan-Meier mean TSP total chromium concentrations by site during MATES IV (2012-2013) and MATES V (2018-2019). Error bars indicate 95% confidence intervals.

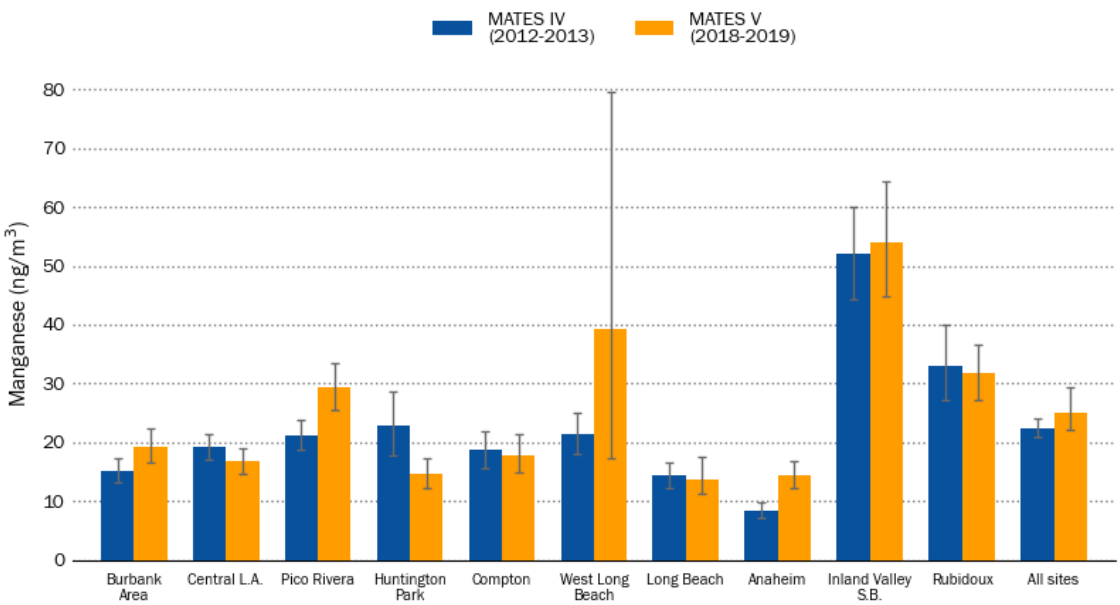

Figure X-12. Kaplan-Meier mean TSP manganese concentrations by site during MATES IV (2012-2013) and MATES V (2018-2019). Error bars indicate 95% confidence intervals.

	Burbank Area*	Central L.A.	Pico Rivera	Huntington Park*	Compton	West Long Beach	Long Beach*	Anaheim	Inland Valley S.B.	Rubidoux	All sites
Arsenic	3	-35	17	-26	-12	60	-5	51	-3	-12	-0
Hexavalent Chromium	-19	-37	-29	-46	-46	4	-23	43	-13	-35	-29
Cadmium	415	-42	16	149	48	507	-61	179	10	348	114
Nickel	-48	-41	-33	-51	-28	16	1	22	55	-28	-17
Lead	30	-32	-20	-39	-23	-29	-27	28	-22	-28	-21
Manganese	27	-13	39	-35	-5	84	-4	72	4	-4	12
Antimony	-30	-11	-13	-11	20	27	-1	83	20	22	4
Chromium	-15	-19	18	-41	-9	27	-21	17	5	-14	-7
Cobalt	-6	-6	46	-20	9	58	105	52	1	-8	19

Figure X-13. Percent change in Kaplan-Meier mean TSP metal concentrations at each station between MATES IV to MATES V. Asterisks indicate station locations that moved between MATES IV and MATES V.

V. Conclusion

The wide range of particulate measurements at fixed sites during MATES V allowed for the evaluation of changes in patterns of particulate pollution in the 6 years since MATES IV. In general, spatial and seasonal trends in $PM_{2.5}$ composition in the South Coast Air Basin remained similar to those observed in MATES IV. One key change in $PM_{2.5}$ composition was the substantial reduction in average elemental carbon concentrations throughout the basin. On a basin scale, toxic metal concentrations generally decreased or remained at similar levels to those measured in MATES IV, with the exception of a significant increase in average cadmium concentration. However, the overall contribution of cadmium to average population-weighted air toxics cancer risk is less than 1%, and contributions from cadmium to chronic non-cancer risk calculated at each monitoring station are also minimal (basin-wide average of 0.6%). Targeted control measures of both local and regional sources of particulate matter will lead to continued improvement in air quality and reduced health risks in the South Coast Air Basin.

VI. References

Agrawal, Harshit, et al. "Primary Particulate Matter from Ocean-Going Engines in the Southern California Air Basin." *Environmental Science & Technology* 43 (2009): 5398-5402.

Air Quality Research Center, University of California, Davis. "Data Validation for the Chemical Speciation Network: A Guide for State, Local, and Tribal Agency Validators." 2019.

Chow, Judith C., Douglas H. Lowenthal, L.-W. Antony Chen, Xiaoliang Wang, and John G. Watson. "Mass reconstruction methods for PM2.5: a review." *Air Quality, Atmosphere & Health* 8 (2015): 243-263.

Pakbin, Payam, Zhi Ning, Martin M. Shafer, James. J. Schauer, and Constantinos Sioutas. "Seasonal and Spatial Coarse Particle Elemental Concentrations in the Los Angeles Area." *Aerosol Science and Technology* 45 (2011): 949-963.

Seinfeld, John H., and Spyros N. Pandis. *Atmospheric Chemistry and Physics: From Air Pollution to Climate Change.* Third Edition. Hoboken, NJ: John Wiley & Sons, Inc., 2016.

South Coast AQMD. "Multiple Air Toxics Exposure Study in the South Coast Air Basin: MATES IV." 2015.